JOURNAL OF AGRICULTURAL AND FOOD CHEMISTRY

Article

Cite This: J. Agric. Food Chem. 2019, 67, 6569−6573

pubs.acs.org/JAFC

Biocompatible Polymers for the Synthesis of Nanosalts via Supramolecular Ion−Dipole Interaction

Sirui Li,[†,‡] Yang Yang,[†,‡] and Kun Liu*[,†,§]

[†]State Key Laboratory of Supramolecular Structure and Materials, Jilin University, Changchun 130012, People's Republic of China

Supporting Information

ABSTRACT: High salt (NaCl) consumption is critical for many healthy problems, e.g., high blood pressure, heart attack, and stroke. Nanosized NaCl particles hold great promise for reducing salt intake; however, they suffered from deliquescence due to their large surface area. We report a facile yet general strategy for the preparation of NaCl nanoparticles (nanosalts) with controllable sizes and moisture resistance property by using biocompatible polymers, such as polyethylene glycol, polyvinylpyrrolidone, polypropylene glycol, polylactic acid, polycaprolactone, and copoly(oxyethylene/oxypropylene/oxyethylene) via supramolecular ion−dipole interaction. The size can be tuned in a range of 100−160 nm by changing the molecular weight or concentration of polymer ligands. Nanosalts protected by polymers showed faster dissolution rate and better moisture resistance compared with microsized NaCl particles without polymer ligands. This work promotes the future development of nanosalts for food and industrial applications to improve human health.

KEYWORDS: *biocompatible polymers, NaCl nanocrystals, moisture resistance, supramolecular, ion−dipole interaction*

Downloaded via CHANGCHUN INST OMP on June 22, 2020 at 06:19:13 (UTC).
See https://pubs.acs.org/sharingguidelines for options on how to legitimately share published articles.

INTRODUCTION

High intake of salt (NaCl) contributes to high blood pressure and increases the risk of cardiovascular disease and stroke.[1] The maximum level of salt intake recommended by the World Health Organization is 5 g/day for adults. However, most people consume 9−12 g/day, which is twice the standard intake in certain areas. Reducing salt intake could therefore be an important target for improving public health. The high intake of salt is partially caused by their large sizes (millimeter scale) and low compatibility with food matrix. It has been showed that 70−95% of salt powders remain in the food matrix even after being swallowed but without being perceived.[1,2] Reducing the particle size of salt could increase its surface area, leading to an increased dissolution rate in saliva and more efficient transfer of Na ions to taste buds and, hence, a saltier perception of foods.[3−7]

A number of strategies have been attempted to fabricate micro- or nanoscale NaCl,[8−12] including grinding,[13−15] laser ablation,[13,16] vapor drying,[17−19] nanospray drying,[7] electrospray techniques,[20] and a cryochemical method.[21] In addition, different morphologies of NaCl crystals with uniform microscale sizes have been synthesized by controlled precipitation of NaCl in organic solvents.[22,23] However, the NaCl particles produced through these methods would be difficult to store due to the caking property of NaCl as a result of the lack of surface ligand protection, which limited its further application. In order to balance the property of fast dissolution rate and deliquescence proof capability, a polymer layer coating on the NaCl nanoparticles (NPs) should be highly desired.

Herein, we report a facile yet general strategy for the preparation of NaCl NPs (nanosalts) with controllable size. Nanosalts with average sizes in the range of 100−160 nm were synthesized by controlled precipitation of NaCl in poor organic solvents under ultrasonication in the presence of biocompatible polymers, e.g., polyethylene glycol (PEG). The PEG ligands are binding the surface of nanosalts via supramolecular ion−dipole interaction, provide good dispersibility and moisture resistance in humid environment with a relative humidity (RH) of up to 75%, and meanwhile do not affect the dissolution rate. The synthesized nanosalts exhibit a faster dissolution rate and better moisture resistance than microsized salt without protection by polymers. This synthetic method is also adaptable for other biocompatible polymers, such as polyvinylpyrrolidone (PVP), polypropylene glycol (PPG), polylactic acid (PLA), polycaprolactone (PCL), and copoly(oxyethylene/oxypropylene/oxyethylene) (Pluronic F127).

MATERIALS AND METHODS

Materials. Sodium chloride (NaCl, AR, ≥99.5%), methanol (AR, ≥99.5%), and dichlormethane (DCM, AR, ≥99.5%) were purchased from Beijing Chemical Works. Tetrahydrofuran (THF, HPLC grade, ≥99.9%) was purchased from Fisher Chemical. Trimethyl carbinol (AR, ≥99.5%) and PEG (number average molecular weight, M_n = 4.0 and 6.0 kg/mol) were purchased from Tianjin Huadong Chemical Works. PEG (M_n = 2.0, 5.0, and 10.0 kg/mol), Pluronic F127 (M_n = 12.0 kg/mol), and PVP (M_n = 58.0 kg/mol) were purchased from Sigma-Aldrich. Food-grade PEG (M_n = 10.0 kg/mol) was purchased from MIKI Corp. in Japan. PLA (M_n = 40.0 kg/mol) and PCL (M_n = 80.0−100.0 kg/mol) were synthesized from the Changchun Institute of Applied Chemistry. All chemicals were used in the experiments without further purification.

Synthesis of Nanosalts@PEG. For a typical synthesis of nanosalts, a NaCl-saturated methanol solution (170 μL, 0.17 M) was rapidly injected into 5.0 mL of a PEG solution in THF (10.0 kg/mol, 100 mg/mL) under sonication at room temperature. The solution became white and cloudy immediately, indicating formation of nanosalts (average size of 117.0 ± 17.3 nm). The nanosalts were then washed four times with THF at 8000 rpm for 10 min.

Received: March 28, 2019
Revised: May 10, 2019
Accepted: May 21, 2019
Published: May 22, 2019

© 2019 American Chemical Society

DOI: 10.1021/acs.jafc.9b01927
J. Agric. Food Chem. 2019, 67, 6569−6573

Synthesis of Nanosalts with Other Biocompatible Polymers. The procedures were the same as the synthesis of the nanosalts@PEG described above, except for PVP in trimethyl carbinol (M_n = 58.0 kg/mol, 50 mg/mL), PPG in tetrahydrofuran (M_n = 4.0 kg/mol, 50 mg/mL), PLA in dichloromethane (M_n = 40.0 kg/mol, 50 mg/mL), PCL in dichloromethane (M_n = 80.0−100.0 kg/mol, 50 mg/mL) and F127 in tetrahydrofuran (M_n = 12.0 kg/mol, 50 mg/mL).

Characterization. Transmission electron microscopy (TEM) images were acquired by a Hitachi-800 transmission electron microscope operating at 175 kV on carbon-coated TEM grids. High-resolution transmission electron microscopy (HRTEM) images were taken on a JEM-2100F at 200 kV, and point-to-point resolution of this HRTEM is 0.5 nm. Scanning electron microscopy (SEM) images were obtained in a Hitachi SU2080 scanning electron microscopy. X-ray diffraction (XRD) was obtained by a PANalytical B.V.-Empyrean operating at 60 kV and 60 mA, using Cu Kα target. Fourier transform infrared (FTIR) spectra were measured by a Bruker VERTEX 80 V spectrometer; the samples were dropped on the KBr substrate. X-ray photoelectron spectroscopy (XPS) was obtained by PREVAC sp.z.0.0 R3000 high resolution ultraviolet photoemission spectroscopy; the samples were dropped on ITO and dried at room temperature. Due to the poor electrical conductivity of NaCl, the sample of nanosalts@PEG should be thin enough.

RESULTS AND DISCUSSION

Characterization of NaCl NPs. NaCl NPs were synthesized by mixing a methanol solution of NaCl with a poor solvent for NaCl (i.e., THF) under ultrasonication in the presence of PEG (analytic grade: Figures 1 and S1; food grade: Figure S2) or

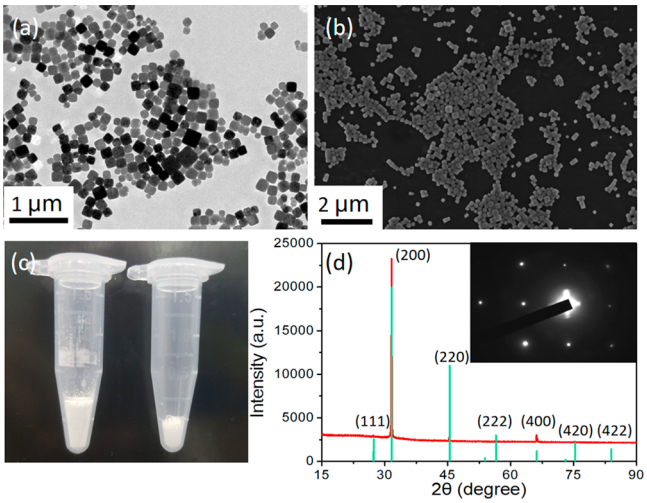

Figure 1. (a) TEM and (b) SEM image of nanosalts. (c) Optical photo of nanosalts (left) and microsized salt (right) with the same weight of 100 mg. (d) XRD patterns of the NaCl nanocubes (red) and bulk NaCl crystals (green). (Inset of d) SAED pattern of an individual nanosalt.

other biocompatible polymers, which allow controlled crystallization of NaCl into colloidal NPs. Figure 1a and 1b shows the representative transmission electron microscopy (TEM) and scanning electron microscopy (SEM) images of the as-prepared cubic nanosalts using this approach with PEG ligand, respectively. The energy-dispersive spectrum mapping analysis of NPs confirms a uniform distribution of Na and Cl across the whole NP (Figure S3). These NaCl nanocubes have a slightly truncated cubic shape with a mean edge length of 151.7 ± 29.0 nm. The dynamic light scattering (DLS) result of nanosalts in THF solution shows a single sharp peak with an average hydrodynamic diameter of 197.8 ± 24.8 nm (Figure S4a), which is consistent with the TEM results. Figure 1c shows the macroscopic solid powder of nanosalts (average size of 151.7 ± 29.0 nm) and microsized NaCl (average size of 106.6 ± 43.2 μm) with the same weight of 100 mg. Compared with microsized salts, nanosalts are fluffier and 2.5 times larger in volume. The content of PEG in nanosalts is about 1.2 wt % as determined by the thermogravimetric analysis data (Figure S4b), which is equal to a grafting density of 0.08 chains/nm^2, similar to the value of PVP-grafted silver NPs.[24]

The crystalline nature of the NaCl nanocubes was confirmed by X-ray diffraction (XRD). Figure 1d shows the XRD pattern of nanosalts synthesized with PEG. The XRD peaks of 31.61, 45.36, and 66.16 degrees are assigned to the (200), (220), and (400) crystallographic planes, respectively. Remarkably, the peak intensity ratios of (200)/(111) and (400)/(111) are much higher than those of bulk crystals, indicating that the nanosalts are abundant with {100} facets, which is consistent with the TEM observation. The cubic shape of NaCl nanocrystal is attributed to the preferential binding of PEG to {100} facets compared to other facets, resulting in suppression of the growth in the ⟨100⟩ directions. Moreover, the square symmetry of the selected area electron diffraction (SAED) pattern further confirms that the NaCl nanocube synthesized with PEG is a single crystal bounded mainly by {100} facets, matching well with the XRD results.

Size Control. PEG ligand is critical for the preparation of nanoscale NaCl particles. Without PEG, NaCl particles (an average size of 51.9 ± 9.8 nm) were formed using the same method, but they rapidly fused into large aggregates with irregular morphology within 30 min after being synthesized (Figure S5). Both the molecular weight and the concentration of PEG ligands play important roles in controlling the growth of nanosalts. Tuning the molecular weight of PEG allows for control of the interaction strength between PEG ligand and NaCl, which subsequently affects the nucleation number of NaCl in the initial stage of the growth process and, consequently, controls the dimensions of the produced nanosalts. For example, under the same concentration of PEG (50 mg/mL), the size of nanosalts can be tuned from 160.0 ± 27.8 to 100.0 ± 12.1 nm by increasing the molecular weight of PEG from 2.0 to 5.0 kg/mol (Figure 2a−c). However, the average size of nanosalts did not

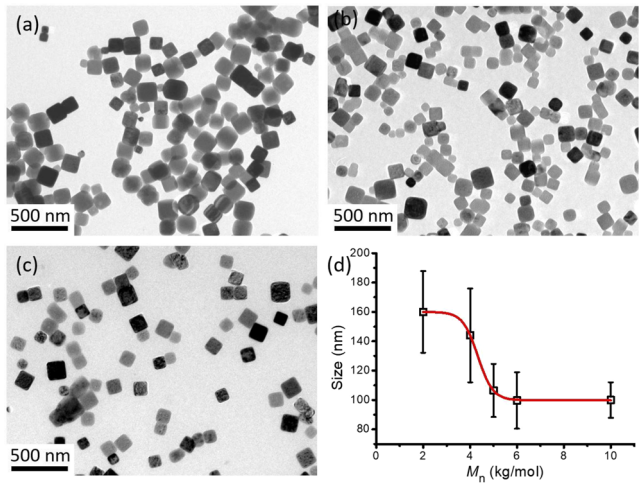

Figure 2. TEM images of the NaCl nanocubes synthesized with different molecular weights of PEG: (a) 2.0, (b) 5.0, and (c) 10.0 kg/mol. (d) Size control curve of NaCl nanocubes with different molecular weights of PEG.

DOI: 10.1021/acs.jafc.9b01927
J. Agric. Food Chem. 2019, 67, 6569−6573

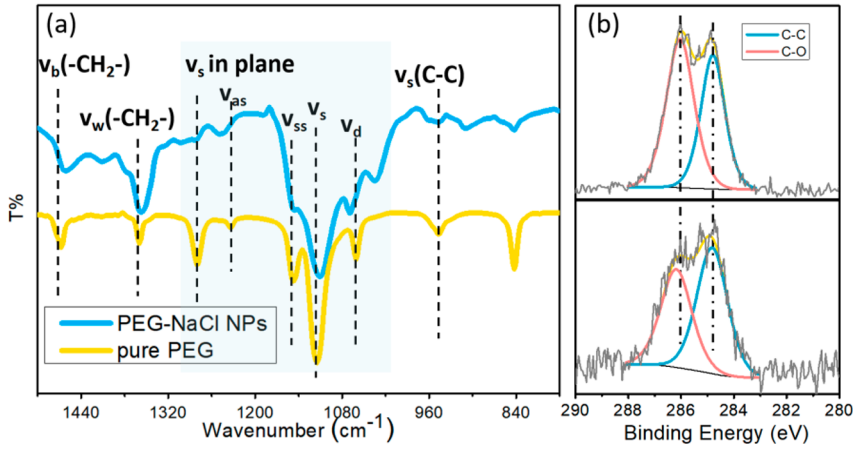

Figure 3. (a) FTIR spectra of pure PEG (yellow) and nanosalts (blue). (b) C 1s XPS spectra for pure PEG (top) and nanosalts@PEG (bottom).

show significant changes when the molecular weight was increased from 5.0 to 10.0 kg/mol (Figure 2d). When the molecular weight of PEG was smaller than 2.0 kg/mol, the NaCl nanocrystals synthesized with PEG (M_n = 1.0 kg/mol) were more round-shaped and aggregated (Figure S6). Similarly, the size of nanosalts can be also tuned by regulating the concentration of PEG. For PEG with M_n of 10.0 kg/mol, the size of the nanosalts increased from 100.4 ± 18.8 to 151.7 ± 29.0 nm by increasing the concentration of PEG from 50 to 250 mg/mL (Figure S7). With a lower concentration of PEG, i.e., 40 mg/mL, there were not enough ligands for the protection and dispersion of nanosalts, leading to the fusion and aggregation of nanosalts (Figure S8). With a higher concentration of PEG, the nucleation of nanosalts was hindered by the high viscosities of the solution, resulting in formation of larger particles eventually. These results suggest that the size of nanosalts can be well controlled by PEG ligands.

Supramolecular Ion−Dipole Interaction. We further studied the bonding interaction between PEG and nanosalts. It is well known that there is a supramolecular ion−dipole interaction between crown ethers and metal ions, including Li^+, Na^+, K^+, etc.[25,26] Cation−polyether complexes are governed by ion−dipole interaction between the cations and the electronegative oxygen atoms of the polyether rings. Characteristic changes in the infrared spectra of the aromatic polyethers had been used to determine the nature of the complexes. In the present study, the ion−dipole interaction between PEG and nanosalts was also characterized by Fourier transform infrared spectroscopy (FTIR) (Figures 3a and S9). Compared with the peaks of pure PEG, the deformation vibration (V_d) and asymmetric stretching vibration (V_{as}) peaks of C−O−C bonds in nanosalts were weakened in intensity and red shifted from 1061 and 1233 cm^{-1} to 1070 and 1248 cm^{-1}, respectively. These changes of the V(C−O−C) bond confirmed the binding interaction between sodium ions and the ether oxygen atoms in PEG segments.[27] Meanwhile, the bending vibration (V_b) and wagging vibration (V_w) peaks of methylene (−CH_2−) in nanosalts were increased in intensity and blue shifted from 1360 and 1467 cm^{-1} to 1357 and 1462 cm^{-1}, respectively. This result indicates that there is less restriction of −CH_2− from the oxygen atoms because they were bonded with sodium ions.[25]

X-ray photoelectron spectroscopy (XPS) analysis further confirmed the ion−dipole interaction between nanosalts and PEG. Compared with that of pure PEG, the binding energy of the C−O bond of the PEG absorbed on nanosalts was found to shift from 286.01 eV to a higher value of 286.19 eV (Figure 3b). This result indicates that the O atom in the C−O bond possesses a lower electron density after absorbing onto the NaCl surface by sharing the electrons with sodium ions, implying a strong ion−dipole interaction between nanosalts and PEG. Meanwhile, the binding energy of Na 1s was reduced from 1072.41 to 1072.15 eV (Figure S10), suggesting a higher electron density when interacting with PEG. Both XPS and FTIR results verify the ion−dipole interaction between PEG and nanosalts.

Rapid Dissolution. Nanosalts possess a fast dissolution rate due to their large specific surface area.[28] We demonstrate the superior dissolution rate of nanosalts@PEG (average size of 120.3 ± 28.4 nm) compared with that of microsized NaCl particles (average size of 106.6 ± 43.2 μm). As shown in Figure 4a, the dissolution of these two types of salts (0.2 mg) in deionized water (10 mL) was monitored by the change of electrical conductivity of the solutions. The conductivity evolution curve for the nanosalts (orange line) showed a small lag phase as a result of the protection of PEG ligands (in the beginning of 2−3 s) followed by a very steep slope and plateaued at about 7 s. The dissolution process of microsized salts shows a similar conductivity evolution curve (blue line) but with a much slower rate. It took more than 20 s for the dissolution process to reach the plateau. The nanosalts show a much faster dissolution

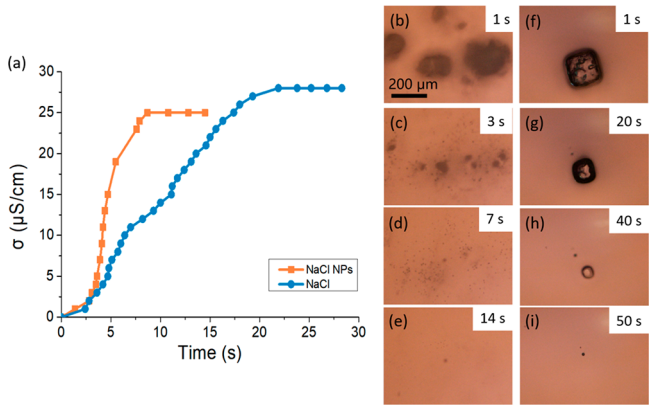

Figure 4. (a) Conductivity curves of the solutions during the dissolution of nanosalts (orange line) and microsized NaCl (blue line). (b−i) Optical microscope images of the dissolution process of nanosalts (b−e) and microsized NaCl (f−i) at different dissolution times as indicated in the upper-right corners.

DOI: 10.1021/acs.jafc.9b01927
J. Agric. Food Chem. 2019, 67, 6569−6573

rate than the microsized salt particles. It should be noted that the smaller final conductivity of nanosalts solution was caused by the presence of 1.2 wt % of PEG ligand in the nanosalts.

The dissolution processes of these two types of salts were also visualized using an optical microscope, which confirmed rapid dissolution of the nanosalts (Figure 4b–i, Videos S1 and S2). A microsized particle and nanosalts with the same weight (0.02 mg) were placed on an aqueous film (1.5 × 2.5 cm) consisting of 50 μL of deionized water. It was observed that though the nanosalts were aggregated in the solid state, they became dispersed and dissolved immediately upon contacting the aqueous film. The whole process took less than 14 s, which was much faster than that of microsized NaCl (50 s). The final spots in Figure 4e and 4i were the bubbles produced during the dissolution processes. The rapid dissolution property could play an important role in food and industrial applications.

Moisture Resistance. Nanosalts exhibit improved moisture resistance by the protection of the PEG ligand. NaCl is known to deliquesce above a RH of 75%.[29] For example, when exposed to a RH of 75%, the microsized salts without ligands were dissolved and recrystallized within 30 min (Figure 5a–c). In contrast,

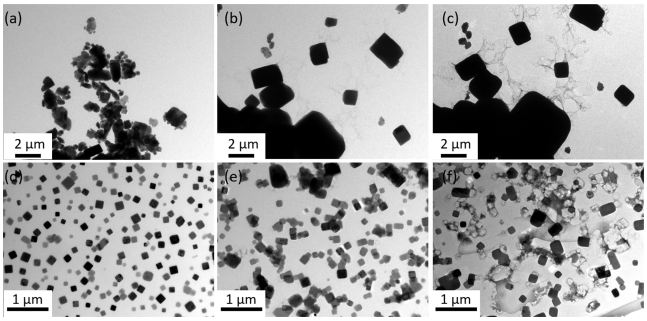

Figure 5. TEM images of PEG-coated nanosalts and microsized salts without ligands at RH of 75%: (a) microsized salts, 0 h, (b) microsized salts, 0.5 h, (c) microsized salts, 8 h, (d) nanosalts@PEG, 0 h, (e) nanosalts@PEG, 78 h, and (f) nanosalts@PEG, 116 h.

nanosalts coated with PEG maintained their nanosized structure for up to 78 h, even if there was some degree of deliquescence (Figure 5d and 5e), and then completely deliquesced after 116 h (Figure 5f). This result indicates that the PEG protection can effectively improve the moisture resistance of nanosalts by restraining the penetration of water molecules through the PEG shell. Below a RH of 75%, the nanosalts were able to retain their nanoscale structure up to the hygroscopic saturation point (Figure S11). The remarkable improvement of moisture resistance will facilitate their storage and transportation.

Nanosalts with Different Biocompatible Polymers. Encouraged by the successful preparation of well-dispersed nanosalts with PEG, we further employed a series of biocompatible polymers which are harmless to the human body or easily degraded by organisms, including PVP (M_n = 58.0 kg/mol), PPG (M_n = 4.0 kg/mol), PLA (M_n = 40.0 kg/mol), PCL (M_n = 80.0–100.0 kg/mol), and copolymer F127 (M_n = 12.0 kg/mol) with the functional group of C–O, to prepare the nanosalts with different surface properties. These polymers exhibit different hydrophilicity, endowing the nanosalts with different moisture resistance properties but not affecting their dissolution property. By using the same approach, nanosalts@PVP (average size of 292.8 ± 63.7 nm), nanosalts@PPG (average size of 89.7 ± 22.9 nm), nanosalts@PLA (average size of 88.1 ± 16.3 nm), nanosalts@PCL (average size of 102.2 ± 26.0 nm), and nanosalts@F127 (average size of 78.2 ± 14.6 nm) were synthesized in good solvents for polymer ligands (50 mg/mL), i.e., trimethyl carbinol for PVP, tetrahydrofuran for PPG and F127, and dichloromethane for PLA and PCL (Figure 6a–d

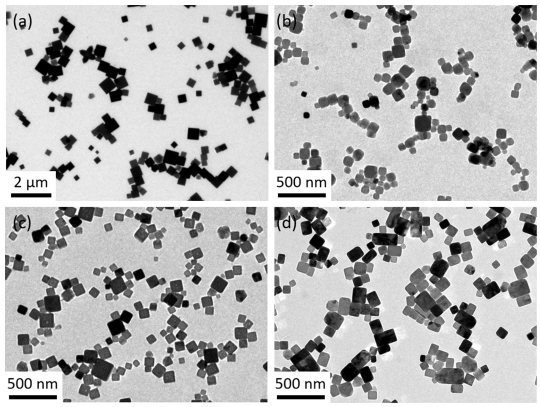

Figure 6. TEM images of the NaCl nanocrystals synthesized with different biocompatible polymers: (a) PVP, (b) PPG, (c) PLA, and (d) PCL.

and Figure S12). These results suggest that this strategy is versatile for preparation of nanosalts with different polymer ligands and therefore applicable for actual production in a broad range.

CONCLUSIONS

In summary, we developed a facile method for the synthesis of size-controlled nanosalts with biocompatible polymers. The size of the produced nanosalts can be fine tuned by the molecular weight or the concentration of polymer ligands. We also demonstrate that the polymer ligands interact with NaCl through ion–dipole supramolecular interaction. Remarkably, nanosalts possess a faster dissolution rate as a result of their relatively large surface area and better moisture resistance owing to the protection of PEG. This work paves the path for application of nanosalts in food and industrial fields.

ASSOCIATED CONTENT

Supporting Information

The Supporting Information is available free of charge on the ACS Publications website at DOI: 10.1021/acs.jafc.9b01927.

High-resolution TEM image of a nanosalt particle with a layer of PEG surface ligand; TEM image of NaCl nanocubes synthesized with food-grade PEG; mapping and energy-dispersive spectroscopy (EDS) analysis of NaCl NP; dynamic light scattering (DLS) data of NaCl nanosalts@PEG according to number percent, and thermogravimetric analysis (TGA) data of NaCl nanosalts@PEG; as-synthesized NaCl nanoparticles without PEG using the same method and the same sample after 30 min of storage in air; TEM image of NaCl nanocubes synthesized with PEG; TEM images of the NaCl nanocubes synthesized with different concentration of PEG, and size control curve of NaCl nanocubes with different concentrations of PEG; TEM image of NaCl nanocrystals synthesized with PEG; Fourier transform infrared spectroscopy (FTIR) of pure PEG and nanosalts@PEG; Na 1s X-ray photoeletron spectroscopy (XPS) spectra for pure PEG and nanosalts@PEG;

DOI: 10.1021/acs.jafc.9b01927
J. Agric. Food Chem. 2019, 67, 6569–6573

nanosalts@PEG and grinded microsized salts without ligand at a relative humidity (RH) of 43%; TEM image of NaCl nanocubes synthesized with F127 (PDF)

Dissolution process of microsized NaCl (MP4)

Dissolution process of NaCl nanoparticles (MP4)

AUTHOR INFORMATION

Corresponding Author

*E-mail: kliu@jlu.edu.cn.

ORCID

Kun Liu: 0000-0003-2940-9814

Present Address

§K.L.: State Key Laboratory of Applied Optics, Changchun Institute of Optics, Fine Mechanics and Physics, Chinese Academy of Sciences, Changchun 130012, People's Republic of China.

Author Contributions

‡S.L. and Y.Y. contributed equally to this work.

Funding

K.L. gratefully acknowledges financial support from the National Natural Science Foundation of China (21534004, 21674042, 21474040). K.L. thanks the funding supported by the Program for JLU Science and Technology Innovative Research Team (JLUSTIRT2017TD-06).

Notes

The authors declare no competing financial interest.

REFERENCES

(1) Quilaqueo, M.; Duizer, L.; Aguilera, J. M. The Morphology of Salt Crystals Affects the Perception of Saltiness. *Food Res. Int.* **2015**, *76*, 675−681.

(2) Phan, V. A.; Yven, C.; Lawrence, G.; Chabanet, C.; Reparet, J. M.; Salles, C. In Vivo Sodium Release Related to Salty Perception during Eating Model Chesses of Different Textures. *Int. Dairy J.* **2008**, *18*, 956−963.

(3) Yi, C.; Tsai, M.-L.; Liu, T. Spray-dried Chitosan/Acid/NaCl Microparticles Enhance Saltiness Perception. *Carbohydr. Polym.* **2017**, *172*, 246−254.

(4) Chokumnoyporn, N.; Sriwattana, S.; Prinyawiwatkul, W. Saltiness Enhancement of Oil Roasted Peanuts Induced by Foammat Salt and Soy Sauce Odour. *Int. J. Food Sci. Technol.* **2016**, *51*, 978−985.

(5) Rama, R.; Chiu, N.; Da Silva, M. C.; Hewson, L.; Hort, J.; Fisk, I. D. Impact of Salt Crystal Size on In-mouth Delivery of Sodium Perception from Snack Foods. *J. Texture Stud.* **2013**, *44*, 338−345.

(6) Moncada, M. L.; Astete, C. E.; Sabliov, C. M.; Olson, D. W.; Boeneke, C. A.; Aryana, K. J. Influence of Nano-Spray Dried Sodium Chloride on the Physicochemical Characteristics of Surface-Salted Cheese Crackers. *Food Nutr. Sci.* **2017**, *8*, 267−276.

(7) Moncada, M.; Astete, C.; Sabliov, C.; Olson, D.; Boeneke, C.; Aryana, K. J. Nano Spray-dried Sodium Chloride and Its Effects on the Microbiological and Sensory Characteristics of Surface-salted Cheese Crackers. *J. Dairy Sci.* **2015**, *98*, 5946−5954.

(8) Townsend, E. R.; van Enckevort, W. J. P.; Meijer, J. A. M.; Vlieg, E. Polymer versus Monomer Action on the Growth and Habit Modification of Sodium Chloride Crystals. *Cryst. Growth Des.* **2015**, *15*, 5375−5381.

(9) van Enckevort, W. J. P.; Noorduin, W. L.; Graswinckel, S.; Verwer, P.; Vlieg, E. Epitaxy of Anthraquinone on (100) NaCl: A Quantitative Approach. *Cryst. Growth Des.* **2018**, *18*, 5099−5107.

(10) Townsend, E. R.; van Enckevort, W. J. P.; Tinnemans, P.; Blijlevens, M. A. R.; Meijer, J. A. M.; Vlieg, E. Additive Induced Formation of Ultrathin Sodium Chloride Needle Crystals. *Cryst. Growth Des.* **2018**, *18*, 755−762.

(11) Daly, R.; Kotova, O.; Boese, M.; Gunnlaugsson, T.; Boland, J. J. Chemical Nano-Gardens: Growth of Salt Nanowires from Supramolecular Self-Assembly Gels. *ACS Nano* **2013**, *7*, 4838−4845.

(12) Lin, H.-X.; Lei, Z.-C.; Jiang, Z.-Y.; Hou, C.-P.; Liu, D.-Y.; Xu, M.-M.; Tian, Z.-Q.; Xie, Z.-X. Supersaturation-Dependent Surface Structure Evolution: From Ionic, Molecular to Metallic Micro/Nanocrystals. *J. Am. Chem. Soc.* **2013**, *135*, 9311−9314.

(13) Zhilenko, M. P.; Muravieva, G. P.; Ehrlich, H. V.; Lisichkin, G. V. Production of Highly Dispersed Sodium Chloride: Strategy and Experiment. *Russ. J. Appl. Chem.* **2016**, *89*, 857−864.

(14) Cheong, Y. S.; Mangwandi, C.; Fu, J.; Adams, M. J.; Hounslow, M. J.; Salman, A. D. A Mechanistic Description of Granule Deformation and Breakage. *Handb. Powder Technol.* **2007**, *12*, 1055−1120.

(15) Baláž, P.; Achimovičová, M.; Baláž, M.; Billik, P.; Cherkezova-Zheleva, Z.; Criado, J. M.; Delogu, F.; Dutková, E.; Gaffet, E.; Gotor, F. J.; Kumar, R.; Mitov, I.; Rojac, T.; Senna, M.; Streletskii, A.; Wieczorek-Ciurowa, K. Hallmarks of Mechanochemistry: from Nanoparticles to Technology. *Chem. Soc. Rev.* **2013**, *42*, 7571−7637.

(16) Kazakevich, P. V.; Simakin, A. V.; Voronov, V. V.; Shafeev, G. A. Laser Induced Synthesis of Nanoparticles in Liquids. *Appl. Surf. Sci.* **2006**, *252*, 4373−4380.

(17) Sun, M.-X.; Guo, D.-Z.; Xing, Y.-J.; Zhang, G.-M. Visible Laser Induced Positive Ion Emissions from NaCl Nanoparticles Prepared by Droplet Rapid Drying. *Appl. Surf. Sci.* **2012**, *258*, 8758−8763.

(18) Wang, Z.; King, S. M.; Freney, E.; Rosenoern, T.; Smith, M. L.; Chen, Q.; Kuwata, M.; Lewis, E. R.; Pöschl, U.; Wang, W.; Buseck, P. R.; Martin, S. T. The Dynamic Shape Factor of Sodium Chloride Nanoparticles as Regulated by Drying Rate. *Aerosol Sci. Technol.* **2010**, *44*, 939−953.

(19) Mansouri, S.; Chen, X. D.; Woo, M. W. Design of Micron-sized Salt Particles by Ethanol Vapour Drying. *Powder Technol.* **2018**, *323*, 558−562.

(20) Zheng, F.; Wang, D.; Fang, H.; Wang, H.; Wang, M.; Huang, K.; Chen, H.; Feng, S. Controlled Crystallization of Sodium Chloride Nanocrystals in Microdroplets Produced by Electrospray from an Ultra-Dilute Solution. *Eur. J. Inorg. Chem.* **2016**, *2016*, 1860−1865.

(21) Annen, T.; Epple, M. A facile Synthesis of Dispersable NaCl Nanocrystals. *Dalton Trans.* **2009**, *44*, 9731−9734.

(22) Wang, B.; Jin, P.; Yue, Y.; Ji, S.; Li, Y.; Luo, H. Synthesis of NaCl Single Crystals with Defined Morphologies as Templates for Fabricating Hollow Nano/Micro- Structures. *RSC Adv.* **2015**, *5*, 5072−5076.

(23) Nalesso, S.; Bussemaker, M. J.; Sear, R. P.; Hodnett, M.; Lee, J. Development of Sodium Chloride Crystal Size during Antisolvent Crystallization under Different Sonication Modes. *Cryst. Growth Des.* **2019**, *19*, 141−149.

(24) Chen, Z.; Chang, J. W.; Balasanthiran, C.; Milner, S. T.; Rioux, R. M. Anisotropic Growth of Silver Nanoparticles Is Kinetically Controlled by Polyvinylpyrrolidone Binding. *J. Am. Chem. Soc.* **2019**, *141*, 4328.

(25) Pedersen, C. J. Cyclic Polyethers and Their Complexes with Metal Salts. *J. Am. Chem. Soc.* **1967**, *89*, 7017−7036.

(26) Pedersen, C. J. The Discovery of Crown Ethers. *Science* **1988**, *241*, 536−540.

(27) Li, X.; Huang, K.; Xu, Y.; Liu, H. Interaction of Sodium and Potassium Ions with PEO-PPO Copolymer Investigated by FTIR, Raman and NMR. *Vib. Spectrosc.* **2014**, *75*, 59−64.

(28) Utembe, W.; Potgieter, K.; Stefaniak, A. B.; Gulumian, M. Dissolution and Biodurability: Important parameters Needed for Risk Assessment of Nanomaterials. *Part. Fibre Toxicol.* **2015**, *12*, 11.

(29) Langlet, M.; Nadaud, F.; Benali, M.; Pezron, I.; Saleh, K.; Guigon, P.; Metlas-Komunjer, L. Kinetics of Dissolution and Recrystallization of Sodium Chloride at Controlled Relative Humidity. *KONA* **2011**, *29*, 168−179.

DOI: 10.1021/acs.jafc.9b01927
J. Agric. Food Chem. 2019, 67, 6569−6573